ELSEVIER

Earth and Planetary Science Letters 202 (2002) 159–170

EPSL

www.elsevier.com/locate/epsl

Hydrothermal heat flux through aged oceanic crust: where does the heat escape?

Heinrich Villinger *, Ingo Grevemeyer, Norbert Kaul, Jan Hauschild, Marion Pfender

FB Geowissenschaften, Universität Bremen, Klagenfurter Straße, 28359 Bremen, Germany

Received 4 March 2002; received in revised form 21 May 2002; accepted 6 June 2002

Abstract

Recent publications suggest that most of the fluid flow in the upper oceanic crust is channelized through small volumes of rock and vented into the ocean. This implies that at flanks of generally thinly sedimented mid-ocean ridges, focused discharge at the seafloor should be concentrated most likely at outcrops, high-angle normal faults or seamounts. These vents should be associated with a significant heat flow signature. However, only few observations worldwide support this assumption up to now. On our quest for focused fluid exchange between young oceanic crust and the ocean we surveyed a 720 km long and 40–90 km wide off-axis portion of seafloor intersecting the East Pacific Rise near 14°14′S. A wealth of geophysical methods including high-resolution swath mapping bathymetry, single channel seismics, sediment echo sounding, magnetics and heat flow determinations were used. Heat flow data in the tectonic corridor cover crustal ages of 0.3–9.3 Ma. With respect to the conductive plate cooling model the data show the well-known pattern of low values close to the ridge, associated with vigorous hydrothermal circulation of cold seawater through the young upper crust, and a fast recovery to almost lithospheric conductive cooling values at a surprisingly young crustal age of 9.3 Ma. Although the sediment cover is fairly thin, measurements with a 3.6 m violin bow type heat probe were possible almost everywhere within the investigated area. A detailed survey between two large seamounts at 4.5 Ma revealed localized extremely high values of up to 618 mW/m^2 (275% of the expected heat flow) at the foot of the seamount. This is interpreted as a clear indication of focused discharge of hydrothermal fluid. If we, however, relate heat flow normalized by the expected conductive heat loss to the character of igneous basement, heat flow is highest in areas with an almost flat and sedimented basement, and lowest within $\sim$10–20 km of seamounts and other rough basement relief. We therefore hypothesize that the large number of seamounts covering the ocean floors governs a major amount of convective heat loss of aging oceanic lithosphere. © 2002 Elsevier Science B.V. All rights reserved.

Keywords: heat flow; hydrothermal conditions; oceanic crust; seamounts

1. Introduction

At mid-ocean ridges lithosphere is created continuously by seafloor spreading. As lithosphere spreads away from the ridge axis it cools and subsides. This concept was generally supported very

* Corresponding author. Tel.: +49-421-218-4509; Fax: +49-421-218-7163.
E-mail address: vill@uni-bremen.de (H. Villinger).

0012-821X/02/$ – see front matter © 2002 Elsevier Science B.V. All rights reserved.
PII: S0012-821X(02)00759-8

early on by the realization that seafloor heat flow is highest at the ridge crest and decreases with distance and hence plate age [1,2]. Therefore the systematic variation of ocean depth and heat flow became the primary constraint on models of the thermal evolution of the lithosphere [3–5]. However, for young oceanic crust a significant discrepancy exists between the low heat flow measured at the seabed and the much higher values predicted by thermal models of a cooling lithosphere. This energy deficit is thought to reflect the removal of significant amounts of heat from the hot young oceanic crust by circulating cold seawater through it [6]. A spectacular result of this hydrothermal circulation is active hot vents at ridge crests discharging fluids with temperatures up to 400°C. On the ridge flanks the ongoing heat loss of the lithosphere drives the circulation of fluids through the porous upper layers of crust. Here at the much lower temperatures the vigor of hydrothermal circulation is reduced. However, due to the vast areas of the seafloor where such circulation can occur, perhaps 70% of the hydrothermal heat loss is off-axis [7].

In the axial zone, high-temperature fluid venting from open fissures is coupled with high-permeability pathways like fault zones which control fluid circulation and hence the cooling process of very young crust [8]. Within older crust, fluid circulation continues and appears to be controlled by the background permeability, yielding a heat flow pattern which roughly mimics the topography [9–12]. In general, however, heat flow determinations on the ridge flanks reveal values well below the theoretical prediction [7], suggesting that there might be high-permeability conduits through which warm fluids can escape [13]. Evidence for such discharge sites, however, is limited. Davis et al. [14] and Langseth et al. [15] provided geothermal evidence for excess heat over buried abyssal hills on the flanks of the Juan de Fuca Ridge and Costa Rica Rift, respectively. In addition, at the Juan de Fuca Ridge Mottl et al. [16] detected warm fluids seeping out of an outcropping abyssal hill on 3.5 Ma old crust.

The aim of our study is to describe the off-axis hydrogeological system of a thinly sedimented ridge environment – the southern East Pacific Rise (EPR) near 14°S (Fig. 1) – by discussing seafloor heat flow measurements in conjunction with bathymetry. This section of the EPR was chosen as it is thought to represent a typical mid-ocean ridge crest and ridge flank environment, in other words a textbook example, where ridge structures are simple and the sedimentation on the flank is purely pelagic. During legs SO-105 and SO-145 of the German research vessel *Sonne* a geophysical program call EXCO (EXchange between Crust and Ocean) has been carried out on zero-age to 9.3 Ma old crust, including swath mapping bathymetry, seismic reflection surveying, seismic refraction work and detailed heat flow surveys. Leg SO-105 (EXCO I) took place in December 1995 and focussed on regional-scale surveys whereas Leg SO-145 (EXCO II), from December 1999 to January 2000, concentrated on small-scale features, based on results from the previous cruise. During Leg SO-105 the regional heat flow pattern was mapped with 16 heat flow stations, normally comprising three to eight thermal gradient and in situ conductivity measurements; stations were roughly spaced at age intervals of 0.6 Ma, that is, at about 45 km intervals. In contrast to Leg SO-105 and most previous heat flow studies Leg SO-145 investigated in detail very young crust and rough terrain like abyssal hills and seamount flanks. Generally, such areas were avoided in the past because of potential damage to heat probes due to lack of sufficient sediment cover. We used geothermal constraints along with bathymetric data to search for possible vent sites and their relationship to seafloor features.

The data described in this paper are primarily from three areas: area 1 on smooth terrain and very young crust of approximately 0.3 Ma, area 2 again on smooth seafloor but 9.1 Ma in age, and area 3 on rough seafloor close to two seamounts with a crustal age of 4.6 Ma.

2. Geological settings

The southern EPR is a so-called superfast spreading ridge where the plates are pulled apart with a full rate of 150 mm/yr [17]. South of the Garrett fracture zone the southern EPR is uncharacteristically devoid of any transform faults for nearly 1150 km [18] but it is offset by small-scale non-transform discontinuities, like overlapping spreading centers. On-axis, a profound feature is its blocky ridge crest indicating a robust magma supply [19], and off-axis, most prominent is the asymmetric distribution of seamounts. Compared to the Nazca plate to the east, the population of seamounts on the Pacific plate to the west is about twice as high [20,21].

Our survey area was a 720 km long and 40–90 km wide tectonic corridor on the Nazca plate intersecting the southern EPR at about 14°S (Fig. 1). Fig. 2a,b summarizes the basic results based on measurements from ECXO I, whereas Fig. 2c,d contains data collected during ECXO II. Magnetic data, mainly collected during ECXO I, allow an unambiguous identification of the sequences of reversals [21]. In this paper, however, we use a slightly revised interpretation [17], suggesting that since 9.3 Ma the Nazca plate has been drifting with an average half rate of 75 mm/yr. Abyssal hill morphology and seamount distribution along the corridor show a common variation with offset from the ridge crest. Characterizing the abyssal hills in terms of their rms height, the seafloor is roughest at 230–525 km offset [21] (Fig. 2a) at an age of about 4.5 Ma. Within this region seamounts are more abundant and higher than elsewhere in the survey area (Fig. 2b). Heat flow data from EXCO I [12,22] and EXCO II show the well-known pattern of values below the prediction of plate cooling models (Fig. 2d) close to the ridge but recovering quite fast to plate cooling model values. This data set will be discussed later in detail.

3. Geophysical methods

The seafloor topography was surveyed during both cruises with a Hydrosweep swath mapping system [23]. The field records were processed with the MB software [24] and gridded using continuous curvature splines in tension [25]. The resulting digital terrain models have been displayed with GMT software [26]. In total about 35 000 km^2 of seafloor (see Fig. 1) were mapped on the eastern flank. The detailed study areas themselves have a size of about 200 km^2 each and are shown in detail in Fig. 3. Sediment thickness was surveyed with a 16 channel 100 m long hydrophone array that recorded shots of a 1.5 l generator–injector air gun. All 16 analog channels were summed up electronically before analog-to-digital conversion and data acquisition. Seismic data processing includes filtering, deconvolution and time migration. Unfortunately, the time available did not allow us to cover the whole survey area with seismic profiles. Therefore only specific areas could be surveyed in detail (crust of 0–2 Ma, 4.5–5 Ma and 7.5–8 Ma in age). However, the high-quality data allowed us to map the sedimentation thickness as a function of age. Within the first 1 Ma after crustal generation about 8–10 m of sediment was accumulated. Thereafter, sedimentation occurred in general with a rate of 3–5 m/Ma (Fig. 2c) except for an area of unusually thick sediment cover between 1.5 and 2 Ma.

All the geothermal measurements were made with a violin bow probe [27,28], based on the initial design by C. Lister. This instrument measures the temperature gradient with 11 temperature sensors (thermistors), mounted inside a sensor tube which itself is attached to a mechanically robust lance of 3.6 m length. After penetration into the sediment frictional heating creates a heat pulse whose decay is recorded over a period of 7 min. In general, equilibrium temperatures are not reached within this time interval, therefore the decays have to be processed to obtain undisturbed in situ sediment temperatures [29,30]. Every second to third measurement is complemented by an in situ conductivity measurement after the pulsed heat source method [28]. The thermal decay of this calibrated heat pulse allows us to estimate the conductivity at the location of in situ temperature measurements [30]. The results of a single penetration (temperature and thermal conductivity vs. depth) are combined for the calculation of the heat flow, after Bullard [31].

All data from the heat probe were transmitted in real time on board using a coaxial cable connecting the probe with the ship. Measurements along a profile (called station) were made in pogo-style fashion with a spacing of 500–1000 m.

The ship's navigation had errors of less than 10 m due to the availability of DGPS. Navigation of the probe itself with respect to the ship was attempted using a Ultra Short Baseline Array, mounted in the ship's hull, and a transponder, mounted on the wire just above the heat probe. However, results were not entirely satisfactory and resulted in errors of the heat flow measurement position of about 45 m. During SO-105, however, only GPS was available, resulting in a positioning accuracy of 100 m. The data set from both surveys comprises in total 175 geothermal gradient determinations and 72 in situ conductivity measurements. The detailed study areas centered on crust 0.3 Ma, 9.1 Ma and 4.6 Ma old provide nine, eight and 18 penetrations, respectively. To indicate the amount of heat being removed by hydrothermal fluids, we used the term heat flow fraction (HFF), which is the ratio between observed and expected heat flow. Thus, a value of 1 indicates that the measured value is in agreement with the theoretical prediction while lower values indicate that heat has been removed by circulating fluids. On the other hand, higher values indicate excess heat and may suggest fluid venting.

4. Results

In the following we will discuss the heat flow results from each survey area (see Fig. 1) separately but in the same manner. In all cases the measurements were projected onto a profile indicated in Fig. 3a–c. Calculated heat flow values are compared to a simple cooling plate model in the way of a HFF to emphasize the influence of local hydrothermal circulation. The plate model used is the one published by Parson and Sclater [4]:

$$q = 475/\sqrt{t}$$

with heat flow q in mW/m^2 and time t in Ma. Rough estimates of temperatures at the sediment–basement interface are calculated under the assumption of a uniform thermal conductivity

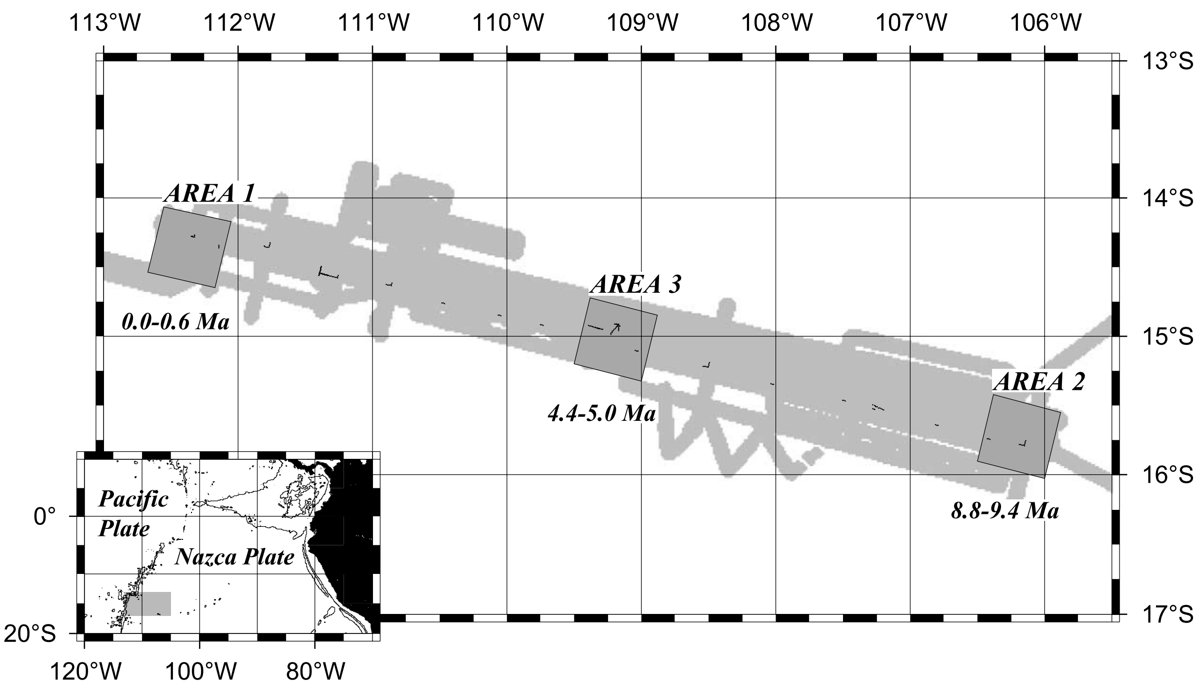

Fig. 1. Location map of the ECXO I and ECXO II investigation area. The gray area has complete bathymetric and magnetic coverage. Areas 1–3 are discussed in detail in the text.

of $k=1$ W/m K and a bottom water temperature T_0 of 1.83°C:

$$T_{\mathrm{Sed-Basement}} = T_0 + (q/k)d$$

with q as calculated heat flow in W/m^2 and sediment thickness d in meters.

Superimposed on all bathymetric data in Fig. 4a–c is a subsidence curve for a cooling half space model:

$$z = 2800 + 360\sqrt{t}$$

with time t in Ma and z in meters. This curve provides the best fit to the bathymetric data [21]. In order to make the results from the three survey areas easily comparable panels a–c of Fig. 4 have the same scale.

Survey area 1 is located on the youngest crust investigated during both cruises. In terms of bathymetry the seafloor is very smooth (Figs. 2a and 3a) with a rms roughness of about 40 m. Seismic techniques and sediment echo sounding could not detect any sediment cover on crust younger than about 0.3 Ma. However, although a gravity corer

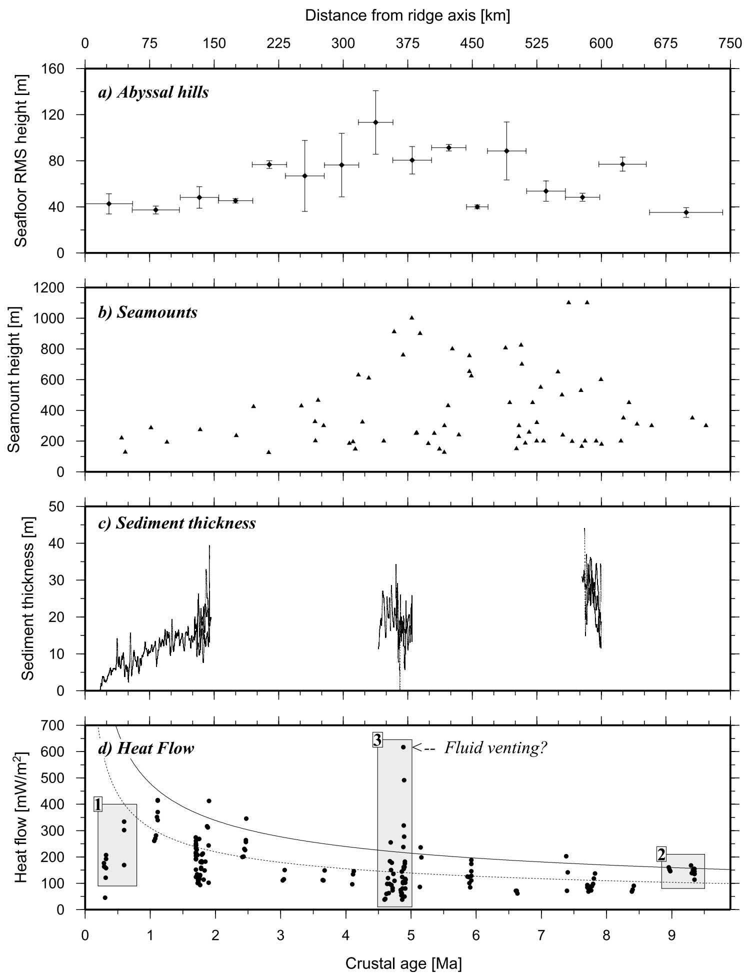

Fig. 2. (a) Seafloor roughness vs. crustal age (for details see Grevemeyer et al. [21]). (b) Seamount height and abundance vs. crustal age. (c) Sediment thickness vs. crustal age, derived from single-channel seismic surveys during EXCO II. (d) Heat flow values vs. crustal age, measured during EXCO I [12] and EXCO II. The solid line is the lithospheric cooling curve of Parson and Sclater [4], the dashed line represents a cooling curve incorporating hydrothermal circulation effects [40].

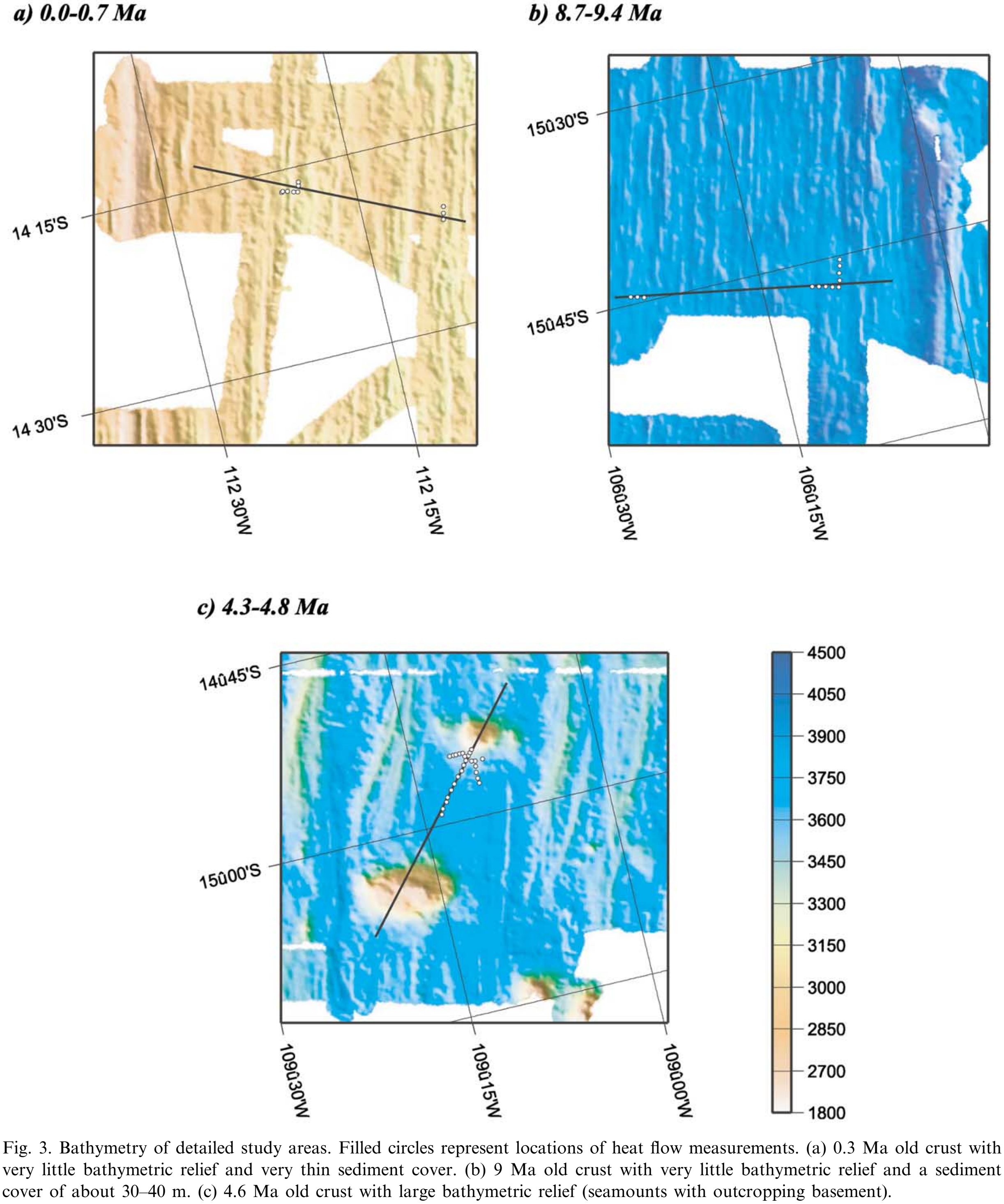

Fig. 3. Bathymetry of detailed study areas. Filled circles represent locations of heat flow measurements. (a) 0.3 Ma old crust with very little bathymetric relief and very thin sediment cover. (b) 9 Ma old crust with very little bathymetric relief and a sediment cover of about 30–40 m. (c) 4.6 Ma old crust with large bathymetric relief (seamounts with outcropping basement).

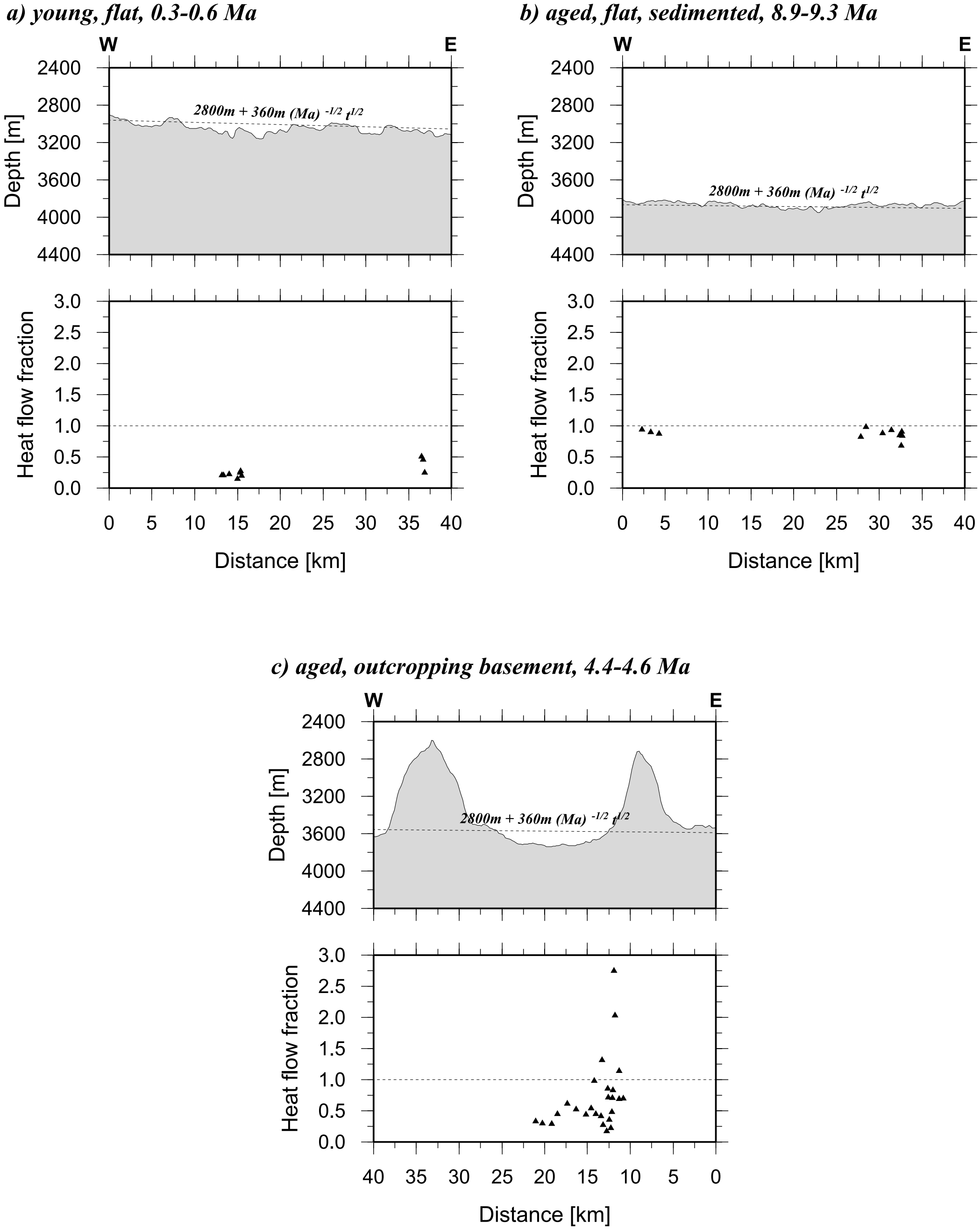

Fig. 4. Bathymetric profile (top) in comparison to HFF vs. distance for the areas 1–3. Values < 1 suggest that heat has been removed by circulating fluids while values > 1 indicate excess heat, perhaps provided by hydrothermal venting.

in this area hit basement it still recovered about 4 m of sediment. At all but at one location all penetrations with the 3.6 m long heat probe provided good heat flow data. We therefore conclude that at least 2–4 m of sediments cover the seabed. All nine successful measurements are projected onto a profile roughly perpendicular to the ridge and are shown in Figs. 2 and 3a. Heat flow fraction (Fig. 4a) varies between 0.15 (130 mW/m^2) and 0.51 (335 mW/m^2). The discrepancy between the observed and model-predicted heat flow suggests that large quantities of heat have been removed by circulating cold seawater, hereby reducing temperatures at the sediment basement interface basically to values slightly above bottom water temperatures (Figs. 2d and 4a).

Seafloor survey at area 2 at the end of the EXCO corridor reveals that the bathymetry is again remarkably smooth (Figs. 2a and 3b). Its rms height is less than 40 m. The interpretation of magnetic data suggests that the volcanic crust is about 9.1 Ma in age. Unfortunately, due to time constraints we were not able to seismically map sediment thickness in this area during Leg SO-145. Sediment echo sounding only provided a few interpretable records. We therefore have to infer sediment thickness. Assuming that the trend of increasing sediment thickness could be interpolated from 6.3 Ma old crust (Fig. 2c) to the 9 Ma old crust sediment thickness is estimated at about 30–40 m. The heat flow values obtained are reasonably constant between 0.68 (107 mW/m^2) and 0.98 HFF (154 mW/m^2), thus heat flow values are close to the trend of the plate cooling model (Figs. 2d and 4b), suggesting that crustal heat loss is possibly governed by thermal conduction alone. Temperatures at sediment–basement interface are slightly elevated to values of about 7–8°C.

Area 3 is located on 4.6 Ma old crust. The survey was conducted in the vicinity of two medium to large sized seamounts (Figs. 3c and 5) aligned approximately parallel to the ridge. Seafloor rms height is >80 m (Fig. 2a). The seismic reflection survey indicates that the sediment thickness decreases from about 20 m in the middle of the profile between the two seamounts to <3 m when approaching the steep flank of the northeastern seamount. Our initial plan to investigate the variation along a complete profile from one seamount to the other failed as sandy sediments prohibited heat probe penetration about half way in between the two edifices. Three heat flow profiles approaching the northeastern seamount were partially successful. Especially on the flanks about 28% of the measurements failed, because the heat probe hit outcropping basement rocks. Neverthe-

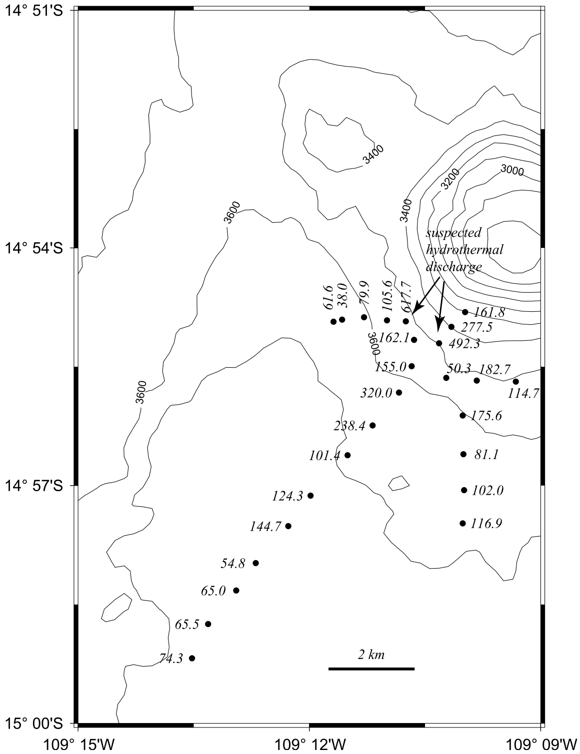

Fig. 5. Detailed results of heat flow survey in the vicinity of a seamount, shown also in an overview of the setting in Fig. 3c. HFFs are shown in Fig. 4c. The numbers represent heat flow values in mW/m^2.

less, in total 18 penetrations provided heat flow values which generally increase toward the seamount. The highest value is 618 mW/m^2, which is 275% of the expected conductive heat loss. The lowest value of 38 mW/m^2 was detected about 4 km away from the seamount top with a HFF of 0.17 (Fig. 4c). Heat flow is generally increasing from a background value around 60–70 mW/m^2 towards the seamount, which can be partially attributed to sediment thinning but values as high as about 500–600 mW/m^2 can only be explained if hydrothermal discharge of fluids at slightly elevated temperatures above background values is present. Temperature anomalies in the bottom water could not be detected which also points to a low temperature discharge. Assuming a heat flow of 600 mW/m^2 temperatures at the sediment–basement interface are in the range of about 14°C under the assumption of a 20 m sediment cover. Attempts to better define the area of high heat flow failed due to the hostile nature of the sedimentary environment (thin sediment cover to bare rock environment) which prevented penetration of the probe. Judging from the two high values at basically identical depth venting seems to be associated with the basal part of the seamount. Groundtruthing the suspected discharge at the seafloor was planned during the cruise using a deep tow camera system incorporating a CTD but had to be cancelled due to operational constraints and is planned at a later date.

5. Discussion and conclusions

Global compilations of marine heat flow data indicate that hydrothermal circulation removes large quantities of heat from the upper crust until oceanic lithosphere reaches an age of about 50–65 Ma (so-called sealing age, after Stein and Stein [7]). This trend can also be observed in heat flow values between crustal ages of 5 and 9 Ma (Fig. 2d). Therefore, the observed heat flow found in area 2 on 9 Ma old crust with HFF values of 0.68–0.98 either contradicts the published sealing age or is just fortuitous. The observed small variations in heat flow could be due to refraction of heat, or – if the basement is isothermal – could easily be interpreted in terms of a variable thickness of sediments of 5–10 m [32], which is not unreasonable with respect to the variability observed in seismic records elsewhere (Fig. 2c).

The simplest explanation to reconcile observations with a model is that there is very little hydrothermal circulation present in the upper crust and cooling occurs mainly by conduction. The decreasing HFF with increasing crustal age could be interpreted as an evolutionary process of decreasing crustal permeability by sealing fractures, fissures or other open voids by secondary mineralization. The clearest support for this hypothesis comes from refraction seismic experiments in the EXCO transect which show a rapid increase of seismic velocities in a crustal time window from 0 to 9 Ma [12], which is in very good agreement with global compilations by [33–35]. In addition, permeability of the uppermost crust (layer 2A) decreases in the same interval by almost three orders of magnitude [13,34,36]. Alternatively exchange of fluids between crust and ocean could be limited even by a thin sediment cover due to the low permeability of deep sea sediments. This covering seal increases in thickness by a factor of about 10 from about 3–4 m in area 1 to about 30–40 m in area 2. The sealing is supported by the analysis of pore fluids from cores taken within area 2, indicating no advective transport [37] between ocean and crust. Sediment cores on younger crust within the EXCO study area show clear indications of flow of hydrothermal fluids from layer 2A into the ocean. It is remarkable and surprising that heat flow data from a completely different environment, the eastern flank of the Juan de Fuca Ridge, show a similar early approach of the lithospheric cooling curve [38].

This view is consistent with the observations from area 3 (Figs. 3c and 4c). In the most general terms the situation defined by the bathymetric and heat flow data can probably best be explained by a model in which fluids reside in a permeable upper crustal 'reservoir' and 'leak' through a generally continuous and low-permeability sediment blanket at isolated locations where basement or other permeability conduits breach the sediment. Such a model of focused discharge has been suggested to explain observations in a sedimented ridge flank setting of the Cascadia Basin [14] and the associated median valley of the Juan de Fuca Ridge [9]. The anomalously high heat flow on the seamount flank (area 3) is probably the result of both conductive and advective effects. Thus, water migrates towards the seamount and dwells out of the flanks and hence transfers heat laterally. In terms of this model the low heat flow values observed at distances of 15–20 km from the seamount suggest fluid flow through a permeable upper crust over the same distance.

If we apply this model to the study areas it suggests that the profound differences in seafloor topography between areas 2 and 3 do control the heat flow pattern. Area 2 revealing heat flow values consistent with the prediction of the plate cooling model is characterized by a nearly flat seafloor. Figs. 3b and 4b indicate that there are no seamounts or large abyssal hills within 30 km of the survey area. Area 3 providing evidence for fluid flow and fluid venting is located in a setting dominated by large abyssal hills and seamounts (Figs. 3c and 4c). This observation is consistent with observations and modeling results which indicate that the off-axis hydrogeological regime is inherently affected by: (i) basal heat flow, (ii) seafloor topography, and (iii) sediment thickness and permeability [9,11,13].

The survey in area 1 (Figs. 2, 3a and 4a) clearly indicates a second form of hydrothermal heat loss. Close to the ridge axis (0–250 km off-axis) the seafloor is very smooth with a rms roughness of 35–50 m and only a few seamounts. Heat flow data, however, suggest that a major amount of heat is being removed. Recharge and discharge through and out of a poorly sedimented seafloor (Fig. 2c) could be caused by both diffuse and focused flow. Jacobson [34] used the term 'open hydrothermal system' for such a setting. As crust ages, the increasing sediment cover may prohibit diffuse flow. However, discharge and recharge of fluids may occur locally and focused [9,12,13], as demonstrated above. Due to the change in the seafloor topography between 250 and 300 km off the ridge axis, the transition is difficult to detect, although the survey in area 2 indicates that it occurs in the first 8–9 Ma.

Area 2 on 9 Ma old crust presents a location which could be interpreted in terms of a closed hydrothermal system [34]. A closed system occurs in areas where the seafloor is continuously covered with several meters of comparatively impermeable sediments and this thick sedimentary blanket may restrict the flow of water through it. However, accumulation of sediment on steep slopes of large abyssal hills and seamounts and their potential for slumping may expose basement rocks and hereby creating open paths for discharge and recharge of fluids. Consequently, the transition to a closed hydrothermal circulation is inherently controlled by the seafloor roughness and the number and size of seamounts on the one hand and the sedimentation rate on the other. This may explain why there is no striking correlation between sediment thickness and the age when hydrothermal circulation ceased [7].

One other major conclusion from our survey is that global data sets are biased to lower values by the distribution of data as noted before by others [40–42]. Generally, rough seafloor, like young crust, flanks of abyssal hills and seamounts have not been investigated in a detailed and systematic way, because of potential damage of heat probes by hitting outcropping basement rocks. Our survey, global data sets [7,39–41] and model calculations by Fisher and Becker [13] suggest that major amounts of heat escaping out of the Earth's interior through the ocean floor have therefore not been sampled and the assessments of the Earth's heat budget may consequently be too low.

Acknowledgements

This work was supported by the German Ministry of Education, Science, Research and Technology (Grants 03G0105A and 03G0145A). We are indebted to the Captains H. Papenhagen and H. Andresen of R/V *Sonne* and their crews for their excellent support and performance at sea. Comments by C.A. Stein and J.-P. Foucher helped to improve the manuscript. We gratefully acknowledge the assistance of B. Heesemann in operating the heat probe. In addition, we thank all the watch standers for cooperation and assistance in data collection at sea. All heat flow data of the EXCO I and EXCO II are available through data base PANGAEA (http://www.pangaea.de).***[AC]***

References

[1] R.P. von Herzen, S. Uyeda, Heat flow through the eastern Pacific ocean floor, J. Geophys. Res. 68 (1963) 4219–4250.

[2] M.G. Langseth, X. LePichon, M. Ewing, Crustal structure of the mid-ocean ridges. 5, Heat flow through the Atlantic ocean floor and convection currents, J. Geophys. Res. 71 (1966) 5321–5355.

[3] E.E. Davis, C.R.B. Lister, Fundamentals of ridge crest topography, Earth Planet. Sci. Lett. 21 (1974) 405–413.

[4] B. Parson, J.G. Sclater, An analysis of the variation of ocean floor bathymetry and heat flow with age, J. Geophys. Res. 82 (1977) 803–827.

[5] C.A. Stein, S. Stein, A model for global variation in oceanic depth and heat flow with lithospheric age, Nature 359 (1992) 123–129.

[6] C.R.B. Lister, On the thermal balance of a mid-ocean ridge, Geophys. J. R. Astron. Soc. 26 (1972) 515–535.
[7] C.A. Stein, S. Stein, Constrains on hydrothermal heat flux through the oceanic lithosphere from global heat flow, J. Geophys. Res. 99 (1994) 3081–3095.
[8] J.B. Corliss, J. Dymond, L.I. Gordon, J.M. Edmond, R.P. von Herzen, R.D. Ballard, K.L. Green, D. Williams, A.L. Brainbridge, K. Craine, T.H. van Andel, Submarine thermal springs on the Galapagos rift, Science 203 (1979) 1073–1083.
[9] E.E. Davis, H. Villinger, Tectonic and thermal structure of the middle valley sedimented rift, northern Juan de Fuca Ridge, Proc. ODP Init. Rep. 139 (1992) 9–41.
[10] H.P. Johnson, K. Becker, R. von Herzen, Near-axis heat flow measurements on the northern Juan de Fuca Ridge: Implications for fluid circulation in oceanic crust, Geophys. Res. Lett. 20 (1993) 1875–1878.
[11] A.T. Fisher, K. Becker, T.N. Narasinham, Off-axis hydrothermal circulation: Parametric test of a refined model of processes at DSDP/ODP site 504, J. Geophys. Res. 99 (1994) 3097–3121.
[12] I. Grevemeyer, N. Kaul, H. Villinger, W. Weigel, Hydrothermal activity and the evolution of the seismic properties of upper oceanic crust, J. Geophys. Res. 104 (1999) 5069–5079.
[13] A.T. Fisher, K. Becker, Channelized fluid flow in oceanic crust reconciles heat flow and permeability data, Nature 403 (2000) 71–74.
[14] E.E. Davis, D.S. Chapman, C.B. Forster, H. Villinger, Heat-flow variations correlated with buried basement topography on the Juan de Fuca Ridge flank, Nature 342 (1989) 533–537.
[15] M.G. Langseth, M.J. Mottl, A. Hobart, A.T. Fisher, The distribution of geothermal and geochemical gradients near Site 501/504, implications for hydrothermal circulation in oceanic crust, Proc. ODP Init. Rep. Part A 111 (1988) 23–32.
[16] M.J. Mottl, G. Wheat, E. Baker, N. Becker, E. Davis, R. Feely, A. Grehan, D. Kadko, M. Lilley, G. Massoth, C. Moyer, F. Sansone, Warm springs discovered on 3.5 Ma oceanic crust, eastern flank of the Juan de Fuca Ridge, Geology 26 (1998) 51–54.
[17] I. Grevemeyer, B. Schramm, C.W. Devey, D.S. Wilson, B. Jochum, J. Hauschild, K. Aric, H.W. Villinger, W. Weigel, A multibeam-sonar, magnetic and geochemical flow-line survey at 14°14′S on the southern East Pacific Rise – insights into the fourth dimension of ridge crest segmentation, Earth Planet, Sci. Lett. 199 (2002) 359–372.
[18] P. Lonsdale, Segmentation of the Pacific-Nazca spreading center, 1°N–20°S, J. Geophys. Res. 94 (1989) 12197–12225.
[19] D.S. Scheirer, K.C. Macdonald, The variation in cross-sectional area of the axial ridge along the East Pacific Rise: evidence for the magmatic budget of a fast spreading ridge, J. Geophys. Res. 98 (1993) 2239–2259.
[20] D.S. Scheirer, K.C. Macdonald, D.W. Forsyth, S.P. Miller, D.J. Wright, M.-H. Cormier, C.M. Weiland, A map series of the southern East Pacific Rise and its flanks, Mar. Geophys. Res. 18 (1996) 1–12.
[21] I. Grevemeyer, V. Renard, C. Jennrich, W. Weigel, Seamount abundances and abyssal hill morphology on the eastern flank of the East Pacific Rise at 14°S, Geophys. Res. Lett. 24 (1997) 1955–1958.
[22] W. Weigel, I. Grevemeyer, N. Kaul, H. Villinger, T. Lüdmann, H.K. Wong, Aging of oceanic crust at the southern East Pacific Rise, EOS Trans. Am. Geophys. Union 77 (1996) 504.
[23] J.A. Grant, R. Schreiber, Modern swathe sounding and sub-bottom profiling technology for research applications: the Atlas Hydrosweep and Parasound systems, Mar. Geophys. Res. 12 (1990) 9–19.
[24] D.W. Caress, D.N. Chayes, Improved processing of Hydrosweep DS multibeam data on the R/V *Maurice Ewing*, Mar. Geophys. Res. 18 (1996) 631–650.
[25] W.H.F. Smith, P. Wessel, Gridding with continuous curvature splines in tension, Geophysics 55 (1990) 293–305.
[26] P. Wessel, W.H.F. Smith, Free software helps map and display data, EOS Trans. Am. Geophys. Union 72 (1991) 441, 445–446.
[27] R.D. Hyndman, E.E. Davis, J.A. Wright, The measurement of marine geothermal heat flow by a multi-penetration probe with digital acoustic telemetry and in situ thermal conductivity, Mar. Geophys. Res. 4 (1979) 181–205.
[28] C.R.B. Lister, The pulse probe method of conductivity measurements, Geophys. J. R. Astron. Soc. 57 (1979) 451–461.
[29] H. Villinger, E.E. Davis, A new reduction algorithm for marine heat flow measurements, J. Geophys. Res. 92 (1987) 12846–12856.
[30] A. Hartmann, H. Villinger, Inversion of marine heat flow measurements by expansion of the temperature decay integral, Geophys. J. Int. 148 (2002) 628–636.
[31] E.C. Bullard, Heat flow in south Africa, Proc. R. Soc. London Ser. A 173 (1939) 474–502.
[32] E.E. Davis, K. Wang, J. He, D.S. Chapman, H. Villinger, A. Rosenberger, An unequivocal case for high Nusselt number hydrothermal convection in sediment-buried igneous oceanic crust, Earth Planet. Sci. Lett. 146 (1997) 137–150.
[33] R.N. Anderson, M.G. Langseth, J.G. Sclater, The mechanism of heat transfer through the floor of the Indian Ocean, J. Geophys. Res. 82 (1977) 3391–3409.
[34] R.S. Jacobson, Impact of crustal evolution on changes of the seismic properties of the uppermost ocean crust, Rev. Geophys. 30 (1992) 23–42.
[35] R.S. Carlson, Seismic velocities in the uppermost oceanic crust: age dependence and the fate of layer 2A, J. Geophys. Res. 103 (1998) 7069–7077.
[36] A.T. Fisher, Permeability within basaltic oceanic crust, Rev. Geophys. 36 (1998) 143–182.
[37] M.J. Mottl, C.G. Wheat, Hydrothermal fluxes on mid-ocean ridge flanks: EXCO II on the eastern flank of the

East Pacific Rise near 14°S (abstract), American Geophysical Union Fall Metting, EOS Trans. Am. Geophys. Union 81 (Suppl.) (1996) F458.

[38] E.E. Davis, D.S. Chapman, K. Wang, H. Villinger, A.T. Fisher, S.W. Robinson, J. Griegel, D. Pribnow, J. Stein, K. Becker, Regional heat flow variation across the sedimented Juan de Fuca Ridge eastern flank: constraints on lithospheric cooling and lateral hydrothermal heat transport, J. Geophys. Res. 104 (1999) 17675–17688.

[39] H.N. Pollack, S.J. Hurter, J.R. Johnson, Heat flow from the Earth's interior: analysis of the global data set, Rev. Geophys. 31 (1993) 267–280.

[40] A.M. Pelayo, S. Stein, C.A. Stein, Estimation of oceanic hydrothermal heat flux from heat flow and depth of mid-ocean ridge seismicity and magma chambers, Geophys. Res. Lett. 21 (1994) 713–716.

[41] C.A. Stein, S. Stein, A.M. Pelayo, Heat flow and hydrothermal circulation, in: S.E. Humphris, R.A. Zierenberg, L.S. Mullineux, R.E. Thomson (Eds.), Seafloor Hydrothermal Systems, AGU Geophys. Monogr. 91 (1995) 425–445.

[42] K. Becker, R.P. von Herzen, Heat flow on the flank of the East Pacific Rise at 21 N, J. Geophys. Res. 88 (1983) 1057–1066.